Revista Eletrônica
Acervo Saúde
Electronic Journal Collection Health ISSN 2178-2091

Parental infection in males causes alterations in the locomotor system in BALB/c mice fetuses

A infecção parental de camundongos machos causa alteração no aparelho locomotor nos fetos de camundongos BALB/c

La infección parental em machos causa alteraciones em el sistema locomotor em fetos de ratones BALB/c

Anderson Arnaldo da Silva[1], Fernanda Carolina Ribeiro Dias[2], Pollyana Oliveira Guimarães[1], Renata Pêssoa Germano[1], Lindomar José Pena[1], Fábio André Brayner[1], Luiz Carlos Alves[1].

ABSTRACT

Objective: To investigate the impact of direct Zika virus infection on male fertility and the body development of mouse offspring. **Methods:** Adult BALB/C mice were divided into three experimental groups: placebo, immunosuppressed, and immunosuppressed/infected. Immunosuppressed males received dexamethasone (50 mg/kg), and the infected group was inoculated with 200 µl (1x10⁴) of ZIKV. After 35 days, the males were mated. Fertility assessments included the number of pregnant females, fetal viability, losses, and biometric measurements. Fetal body morphometry and analysis of skeletal ossification centers were also performed. **Results:** The infected group exhibited an 85% reduction in the ossification centers of the sternum. No significant differences were observed in other somatic, fertility, or placental parameters. Infection was confirmed by RT-PCR. **Conclusion:** Non-viable spermatozoa may be numerically insignificant or potentially reabsorbed by the epididymis, as no changes in fertility were observed. In terms of offspring development, the ZIKV-infected group exhibited skeletal alterations, suggesting a possible delay in locomotor system development.

Keywords: Viral infection, Zika virus, Male fertility, Fetal development.

RESUMO

Objetivo: Investigar o impacto da infecção direta pelo vírus Zika na fertilidade masculina e no desenvolvimento corporal da prole de camundongos. **Métodos:** Camundongos Balb/c adultos foram divididos em três grupos: placebo, imunossuprimido e imunossuprimido/infectado. Os machos imunossuprimidos receberam dexametasona (50 mg/kg), e o grupo infectado foi inoculado com 200ul (1x10^4) de ZIKV. Após 35 dias, os machos foram acasalados. Para avaliações de fertilidade, foram avaliados o número de fêmeas prenhes, viabilidade fetal, perdas e a biometria. A morfometria corporal dos fetos e a análise dos centros de ossificação esquelética também foram realizadas. **Resultados:** O grupo infectado apresentou redução de

[1] Fundação Instituto Oswaldo Cruz (FIOCRUZ), Recife - PE.
[2] Universidade Federal do Triângulo Mineiro (UFTM), Uberaba – MG.

Funding was provided through a scholarship grant from the Coordination for the Improvement of Higher Education Personnel (CAPES) and the Research Support Foundation of the State of Minas Gerais (FAPEMIG), under financial support grant BPD 00733-22.

SUBMETIDO EM: 7/2025 | ACEITO EM: 8/2025 | PUBLICADO EM: 8/2025

85% nos centros de ossificação do osso esterno. Nos demais parâmetros corporais, de fertilidade e placentários não foram observadas diferenças significativas. A infecção foi confirmada através de RT-PCR. **Conclusão:** Espermatozoides não viáveis podem ser numericamente irrelevantes ou possivelmente são reabsorvidos pelo epidídimo, uma vez que não houve alteração na fertilidade. No desenvolvimento da prole, o grupo infectado pelo ZIKV apresentou alterações esqueléticas, indicando possível atraso no desenvolvimento locomotor.

Palavras-chave: Infecção viral, Vírus zika, Fertilidade masculina, Desenvolvimento fetal.

RESUMEN

Objetivo: Investigar el impacto de la infección directa por el virus del Zika en la fertilidad masculina y en el desarrollo corporal de crías de ratones. **Métodos:** Ratones adultos Balb/c fueron divididos en tres grupos experimentales: placebo, inmunosuprimido e inmunosuprimido/infectado. Los machos inmunosuprimidos recibieron dexametasona (50 mg/kg), y el grupo infectado fue inoculado con 200 µl (1x10⁴) de ZIKV. Después de 35 días, los machos fueron emparejados. Para las evaluaciones de fertilidad, se analizaron el número de hembras preñadas, la viabilidad fetal, las pérdidas embrionarias y la biometría. También se realizaron la morfometría corporal de los fetos y el análisis de los centros de osificación esquelética. **Resultados:** El grupo infectado presentó una reducción del 85 % en los centros de osificación del esternón. No se observaron diferencias significativas en los demás parámetros somáticos, de fertilidad o placentarios. La infección fue confirmada mediante RT-PCR. **Conclusión:** Los espermatozoides no viables podrían ser numéricamente insignificantes o posiblemente reabsorbidos por el epidídimo, dado que no se observaron alteraciones en la fertilidad. En cuanto al desarrollo de la descendencia, el grupo infectado con ZIKV presentó alteraciones esqueléticas, lo que sugiere un posible retraso en el desarrollo del sistema locomotor.

Palabras clave: Infección viral, Virus zika, Fertilidad masculina, Desarollo fetal**.**

INTRODUCTION

Zika virus (ZIKV) is a single-stranded, positive-sense RNA virus with an icosahedral nucleocapsid, primarily transmitted by mosquitoes of the genus Aedes (Diptera: Culicidae), classifying it as an arbovirus (LI G, et al., 2017). In Brazil, one of the regions with extensive viral spread, the primary vector is Aedes aegypti, a species with broad distribution (SANTOS J & MENESES BM, 2017; LAPORTA GZ, et al., 2023). Belonging to the Flavivirus family (ICTV, 2024), ZIKV shares many characteristics with other viruses in this taxon, including its vectors, geographic distribution, and affected populations (SANTOS J & MENESES BM, 2017).

Initially identified in the Zika Forest (Uganda), the virus spread across the Asian continent, with cases reported in Malaysia and Indonesia, and later reached Easter Island, eventually arriving in South America around mid-2015 (BROGUEIRA P & MIRANDA AC, 2017). Upon its arrival, the virus spread rapidly, triggering an epidemic that drew significant attention from public health authorities (BROGUEIRA & MIRANDA, 2017). Health agencies soon identified ZIKV infection as the cause of the exponential rise in microcephaly cases observed during the same period, particularly in the state of Pernambuco, Brazil (WHO, 2015), resulting from maternal infection during pregnancy (DUARTE G et al., 2017).

Following the correlation between ZIKV infection and microcephaly, transplacental transmission was confirmed (WATANABE S & VASUDEVAN SG, et al., 2023). Subsequently, based on clinical evidence and experimental data, additional routes of transmission were identified, such as sexual transmission (URAKI R, et al., 2017). Sexual transmission of ZIKV occurs due to the presence of viral particles in male ejaculate, which use this physiological medium as a vehicle to reach the female reproductive tract (CALVET GA, et al., 2018), which also serves as a site for viral replication (ZHANG Y, et al., 2022). This can lead to alterations in sperm morphology and quality in affected individuals (SILVA AA, et al., 2020).

Although the intrauterine environment and the maternal body interact directly with the fetus through the embryonic annexes (DIMASUAY KG, et al., 2016), male reproductive health can also be a critical factor for

offspring viability (WAI-SUN O, et al., 2006). Partial impairment of the testicular and epididymal environments due to pathological processes can negatively affect sperm quality, increasing the proportion of morphologically abnormal sperm in the ejaculate (VERNET P, et al., 2004). When capable of fertilizing oocytes, these altered spermatozoa are more likely to have an adverse impact on embryo development and implantation (DIMASUAY KG, et al., 2016).

While maternal infection has received greater attention due to the microcephaly outbreaks in countries affected by vector-borne transmission, relatively little is known about the potential effects of ZIKV on the male reproductive system and its possible transgenerational consequences. Notably, viral particles can be detected in semen for several weeks after the resolution of symptoms. Thus, the present study aimed to investigate whether paternal ZIKV infection affects male fertility and whether it can influence offspring development.

METHODS

Animals, ethical considerations and experimental design

BALB/c mice (Mus musculus) were used in this study and maintained at the animal facility of the Aggeu Magalhães Institute. Throughout the experimental procedures, animals were kept under controlled environmental conditions: temperature (22 ± 2°C), a 12-hour light/dark cycle, with autoclaved Purina® chow and filtered water provided ad libitum. All experimental protocols were approved by the Institutional Animal Care and Use Committee of the Aggeu Magalhães Institute (CEUA/IAM), under protocol number 181/2022.

A total of 45 animals were used and divided into three groups (10 females and 5 males per group): placebo male, immunosuppressed male, and immunosuppressed and ZIKV-infected male (**Figure 1**).

Figure 1 – Experimental design.

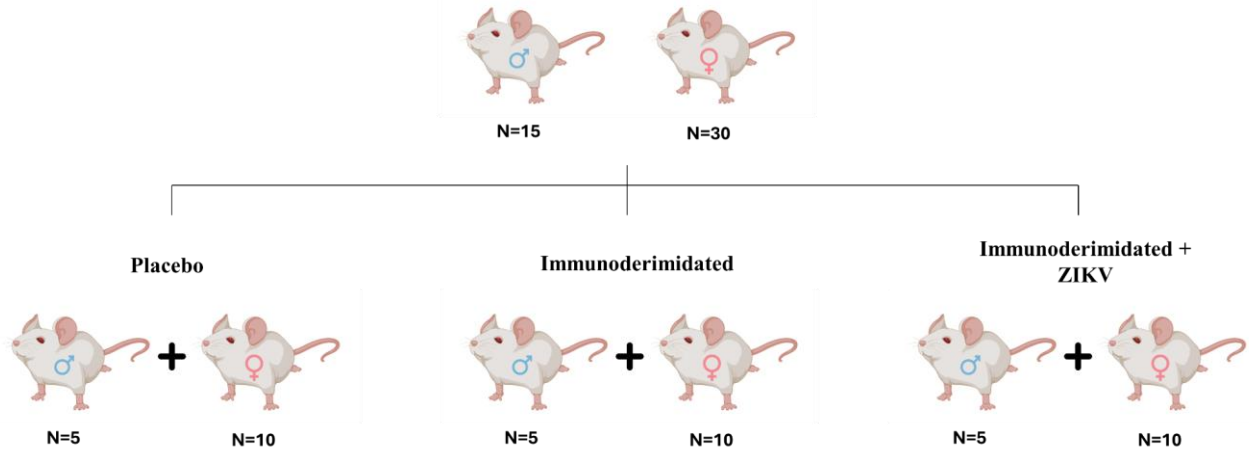

Source: Silva AA, et al., 2025.

Viral culture and infection

ZIKV (strain ZIKV-PE243) was propagated in Vero cell cultures maintained in RPMI 1640 medium (SIGMA), supplemented with 10% heat-inactivated fetal bovine serum (FBS) and 1% penicillin-streptomycin. Viral titration was performed using the TCID₅₀ method, and the concentration of 1×10⁶ was established for animal infection, as defined by Chan et al. (2016). For infection, animals underwent an immunosuppression protocol using dexamethasone phosphate (FARMADEX®) at a dose of 50 mg/kg/day (CHAN JFW, et al., 2016). Male animals in the control (placebo) group were subjected to the same procedures as the experimental groups—including the stress associated with the immunosuppression and infection protocols—but received only the vehicle (PBS), administered in the same volumes and at the same time intervals, without exposure to the immunosuppressive agent or to ZIKV.

Mating procedures

Males were mated 35 days post-infection or post-simulation of infection for a duration of 72 hours, housed in cages with a ratio of 1 male to 2 females. Mating was confirmed by the presence of spermatozoa in vaginal smears (DIAS FCR, et al., 2020; DIAS FCR, et al., 2023). The mating occurred 35 days after infection/simulation to allow sufficient time for the infection to induce sperm damage (SILVA AA, 2020).

Euthanasia and sample collection

Male animals and pregnant females were weighed and anesthetized with sodium pentobarbital (Nembutal®) at a dose of 50 mg/kg in 0.3 mL of injectable water. Once the anesthetic plane was achieved, cardiac puncture was performed to collect blood, which was stored in dry tubes until processing. Fetuses present in the uterine horns of the pregnant females were collected, macroscopically evaluated, weighed, and fixed in 92% ethyl alcohol solution. The uterus, placentas, and ovaries were also weighed using a precision OHAUS® scale (0.000 g) and subsequently fixed in 10% buffered formalin solution for 48 hours.

Processing and analysis of ovary and placentas

The ovaries were dehydrated in ascending concentrations of ethyl alcohol and infiltrated with methacrylate resin (Historesin, Leica Microsystems®, Germany). Subsequently, they were sectioned using a Leica RM2245 semi-automatic rotary microtome (Historesin, Leica Microsystems®, Germany), producing 3 µm-thick sections at 60 µm intervals. The sections were stained with toluidine blue and mounted with Entellan (Merck®).

The placentas had their diameters measured using an analog caliper MTX® (0.02 - 200 mm), obtaining an average between the largest and smallest diameters. Subsequently, the specimens were washed and sectioned at their midpoint along the greatest diameter. The placentas were also dehydrated in ascending ethanol series, cleared in xylene, and infiltrated with histological paraffin. Four-micrometer (4 µm) sections were obtained using a Leica RM2245 rotary microtome and stained with Harris hematoxylin and eosin (H&E) and Masson's trichrome techniques. Panoramic images (image mosaic technique), stained with hematoxylin and eosin, were acquired for histomorphometric analyses. Additionally, the height and total area of the placenta and its two regions—the labyrinth zone and the spongiotrophoblast zone—were evaluated. Sections stained by the Masson's trichrome technique were photomicrographed under a 40x objective in both placental areas for total collagen assessment using ImageJ software (v. 1.50i).

Processing and analysis of fetuses

Head diameter, trunk length, and tail length of the fetuses were measured using an analog caliper MTX® (OLIVEIRA TRDP, et al., 2025). The fetuses were evaluated according to established criteria (Mendes CF, 2012), which included the assessment of macroscopic hemodynamic alterations and malformations. After 48 hours, the fetuses had their skin removed and were processed following the protocol by McLeod MJ (1980). Upon completion of the protocol, the specimens were stored in an aqueous solution of 2% KOH with glycerin (v/v) until analysis.

For bone development analysis, six fetuses per female and six females per group were used. The fetuses were examined under a Zeiss Stemi-305 stereomicroscope (Zeiss, Germany), where ossification centers were counted for the main bone groups: total vertebrae; ribs; sternum; clavicle; scapula; humerus; radius; ulna; thoracic autopod (carpals, metacarpals, and phalanges); pelvic bone (ischium, ilium, and pubis); femur; tibia-fibula; and pelvic autopod (tarsals, metatarsals, and phalanges). At the end of the analysis, averages were calculated per female.

Fertility assessment

Fertility assessment was conducted following the protocols described by Dias FR, et al. (2023). Mating rates were evaluated for both males and females. Pregnancy rates were also determined for each group, along with male fertility rates and rates of embryonic pre-implantation and post-implantation loss. For corpora lutea counting, histological slides of ovarian sections were stained using the histochemical toluidine blue technique, mounted with Entellan® (Merck), and examined under light microscopy.

Detection and quantification of ZIKV viral copy number

Reverse transcription quantitative polymerase chain reaction (RT-qPCR) was performed to confirm infection status in the animals by detecting viral RNA, as well as to quantify the viral copy number present in the serum and testes of parental and F1 generation animals. Tissue fragments were weighed and frozen at -80ºC until RNA extraction. Viral RNA extraction was carried out using the QIAamp Viral Mini Kit (Qiagen), following the manufacturer's instructions. The QuantiNova Probe RT-PCR Kit (Qiagen) was used for the reverse transcription polymerase chain reaction. The primers targeted the sequence encoding the NS5 protein, with the forward primer 5'-AAGCAAAAGGTAGCCGCGCC-3' and reverse primer 5'-TGTCCCAGCCAGCAGTGTCA-3' (Wu et al., 2018). The thermocycler used was the QuantStudio 5 (Applied Biosystems), programmed for 15 minutes at 45ºC, 5 minutes at 95ºC, followed by 45 cycles of 5 seconds at 95ºC and 45 seconds at 60ºC.

RESULTS

Biometry and fertility

Biometric data obtained from the weighing of individuals and evaluated structures showed no significant variations, as did the fertility analyses (**Table 1**).

Table 1 - Body weight, reproductive structures and fetuses (g).

Weight (g)	Grupos experimentais		
	PM	IM	IM+ZIKV
BW	34,20±3,33[a]	34,80±4,35[a]	36,02±2,70[a]
UW	0,82±0,21[a]	0,78±0,15[a]	0,94±0,07[a]
FW	4,17±2,19[a]	3,38±2,51[a]	4,21±2[a]
UW+FW	6,58±3,10[a]	5,98±3,21[a]	7,64±2,70[a]
OW	0,013±0,003[a]	0,013±0,003[a]	0,013±0,001[a]
Corpus luteum	9±1,67[a]	10,33±3,83[a]	8,60±2,96[a]
Implantation sites	7±3,03[a]	9,50±1,83[a]	8,40±2,88[a]
Live fetuses	5,16±3,18[a]	6,66±2,06[a]	7,60±3,28[a]
Aborted fetuses	1,33±1,21[a]	0,66±0,81[a]	0,80±0,83[a]
Resorbed fetuses	0,50±0,83[a]	2,16±2,71[a]	0±0a
Pre-implantation loss	23,81±23,47[a]	4,63±11,34[a]	2±4,47[a]
Pos-implantation loss	31,94±26,57[a]	28,35±24,54[a]	11,94±11,85[a]
Fertility potential	76,19±23,47[a]	95,37±11,34[a]	98±4,47[a]
Fetal viability	68,05±26,57[a]	64,97±20,38[a]	88,05±11,85[a]
Placental index	0,055±0,063[a]	0,064±0,095[a]	0,034±0,023[a]

Legend: PM – Placebo Male; IM – Imunossupressed Male; IM+ZIKV – Imunossupressed Male and infected with ZIKV; CW – Body weigth; UW – Uterine weight; FW – Fetal weight; UW+FW – Uterine and fetal weights. Different letters among experimental groups indicate statistically significant differences (P ≤ 0,05) (Student Newman Keuls test).
Source: Silva AA, et al., 2025.

Viral analysis

The infected male animals used for mating presented detectable viral RNA, as confirmed by RT-PCR, as shown in **Figure 2**:

Figure 2 - Results of viral copy number quantification.

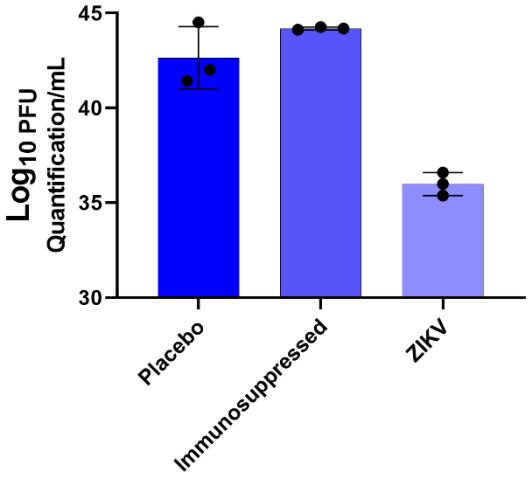

Legend: P ≤ 0,05 (Student Newman Keuls).
Source: Silva AA, et al., 2025.

Fetal biometrics, placental measurements and fetal malformations

In the evaluation of fetuses at 21 days of intrauterine life, differences were observed between placebo and immunosuppressed individuals, but not between immunosuppressed and infected groups (**Table 2**). Measurements related to the fetal skull showed differences in the latero-lateral axis, which was reflected in the cephalic diameter measurement. In both cases, the placebo group differed from the immunosuppressed group, with the latter showing a reduction. No biometric alterations, such as total weight and diameter, were observed in the placentas.

Table 2 - Results of fetal body morphometry (mm).

	Experimental groups		
	MP	**MI**	**MI+ZIKV**
Body segments			
Head			
AA	8,91±1,18[a]	7,07±1,48[a]	7,62±1,19[a]
LA	5,78±0,94[a]	4,29±1,06[b]	8,83±0,77[ab]
HD	7,34±1,05[a]	5,68±1,27[b]	6,72±0,87[ab]
Tronco			
LA	17,84±2,83[a]	13,90±2,73[b]	14,76±1,49[b]
TL	7,45±1,94[a]	5,65±1,44[a]	5,87±1,22[a]
Placental parametes			
Weight (g)	0,131±0,032[a]	0,112±0,011[a]	0,106±0,007[a]
Diameter (mm)	8,85±0,48[a]	8,66±0,47[a]	8,61±0,35[a]
Area (μm²)	10247,1±775	11118±933,2	10648,6±80,57

Legend: PM – Placebo Male; IM – Imunossupressed Male; IM+ZIKV – Imunossupressed Male and infected with ZIKV; AA – Anteroposterior axis; LA – Laterolateral axis; HD – Head diameter; LA – Longitudinal axis; TL – Tail length. Different letters among experimental groups indicate statistically significant differences (P ≤ 0,05) (Student Newman Keuls test).
Source: Silva AA et al., 2025.

Endochondral ossification process in fetuses

Regarding bone development, we observed that the fetal skeleton exhibited alterations in the number of ossification centers (**Figure 3**). In the sternum, animals from the infected group showed a reduction of 85.9% compared to the immunosuppressed group and 96.42% compared to the placebo group (**Table 4**). No significant differences were observed among the groups in the other bones of the axial and appendicular skeleton.

Table 3 - Results of the number of ossification centers by bone group.

Bone groups	Experimental groups		
	MP	MI	MI+ZIKV
TV	30,77±2,54[a]	30,44±3,69[a]	28,11±0,98[a]
Rib	25,52±1,97[a]	24,11±1,84[a]	25,78±0,69[a]
Sternum	2,79±1,44[a]	0,78±0,35[a]	0,11±0,10[b]
Scapula	2±0[a]	2±0[a]	2±0[a]
Humerus	2±0[a]	2±0[a]	2±0[a]
Radius	2±0[a]	2±0[a]	2±0[a]
Ulna	2±0[a]	2±0[a]	2±0[a]
Metacarpals	3,13±3,61[a]	2,33±4,04[a]	0±0[a]
Coxal boné	5,4±1,20[a]	4,8±0,38[a]	4±0,33[a]
Femur	2±0[a]	2±0[a]	2±0[a]
Tibia-fibula	4±0[a]	3,8±0,19[a]	3,89±019[a]
Metatarsals	2,83±3,28[a]	2,39±4,14[a]	0±0[a]

Legend: PM – Placebo Male; IM – Imunossupressed Male; IM+ZIKV – Imunossupressed Male and infected with ZIKV; VT – Total vertebrae. Different letters among experimental groups indicate statistically significant differences (P ≤ 0,05) (Student Newman Keuls test).
Source: Silva AA, et al., 2025.

Figure 3 - Fetal skeleton stained using the clearing technique with bone and cartilage labeling.

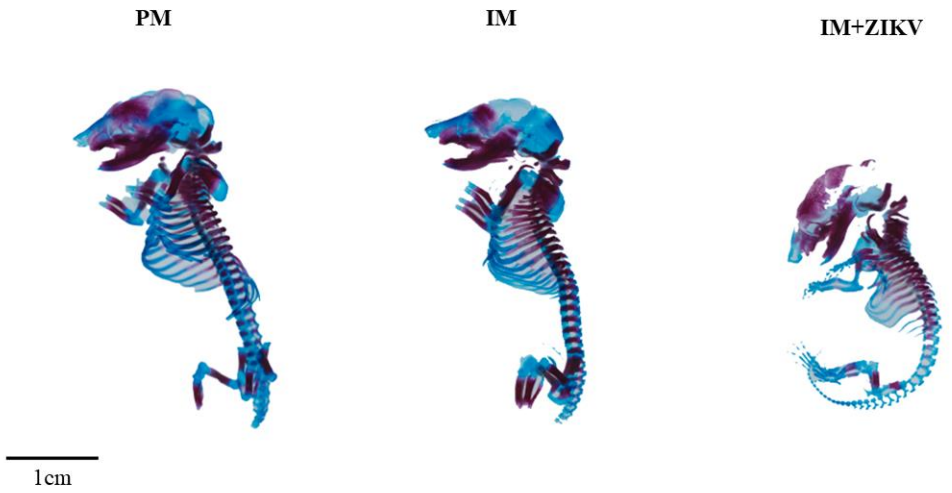

Legend: PM – Placebo Male; IM – Imunossupressed Male; IM+ZIKV – Imunossupressed Male and infected with ZIKV.
Source: Silva, AA et al., 2025.

DISCUSSION

The vertical transmission model of ZIKV infection in mice corroborates human infection cases, demonstrating viral persistence and clinical repercussions, while providing a valuable platform for testing potential therapies and antiviral drugs. This approach broadens possibilities in scientific research, strengthening applicable experimental models for developing strategies to mitigate these infections. Concurrently, it is crucial to monitor and study variants of different ZIKV strains, which may alter infection mechanisms and the efficacy of previously proposed therapies (DOMINGO E, 2016; WU KY, et al., 2016).

The obtained results revealed repercussions in the first-generation offspring, demonstrating that individuals born to infected parents exhibit sequelae such as delayed bone development. This indicates that adverse effects arise not only from maternal infection during gestation but also from paternal infection during spermatogenesis, which negatively impacts embryonic development. Beyond the well-documented effects on the nervous system, the skeletal system is also affected during its formation.

The presence and persistence of ZIKV in the male reproductive system have been confirmed by several recent studies, which report morphological alterations in the gonads and gametes, potentially compromising their functionality (GUO Y, et al., 2024). Although previous reports indicated a reduction in body weight between 5 and 15 days post-infection (dpi) (SHENG GY, et al., 2017; HEBLING MN, et al., 2024), the animals in this study did not exhibit such symptoms, likely due to the infection timing, as animals were mated only at 35 dpi, a period with fewer clinical signs despite reproductive parameter alterations (GOVERO J, et al., 2016; MA W, et al., 2016; SILVA AA, 2020). No changes were observed in the weights of reproductive organs and embryonic annexes, and viral infection was confirmed by RT-PCR in parental generation males.

Although no fertility alterations were detected in these individuals, this may be related to the severity of sperm lesions. Studies with similar post-infection intervals have demonstrated morphological and functional changes in mouse sperm at 35 days post-infection (dpi), including plasma membrane destabilization and modifications in the midpiece and tail (SILVA AA, 2020). Viral and bacterial infections can induce morphological and functional changes in spermatozoa, thereby affecting their viability (GUO Y, et al., 2024). When lesions are severe, damaged spermatozoa are removed from the epididymal lumen, reducing sperm count; however, the remaining spermatozoa are viable and functional (DIAS FCR, et al., 2020; FAISAL K and AKBARSHA MA, 2024). After fertilization, embryogenesis proceeds normally unless significant genetic or morphological alterations impair embryo formation. This biological mechanism is essential for species maintenance, as altered spermatozoa tend to have reduced fertilization success of the secondary oocyte (RAY et al., 2017). However, some studies suggest that, depending on the alteration, modified spermatozoa may occasionally fertilize oocytes (BUSNELLI A et al., 2023). This likely explains the absence of changes in fetal viability, gestational loss, and placental index observed in this study, indicating a reduced impact on fertility at the post-infection time point evaluated, probably due to the severity of spermatic alterations. Even when fertilization occurs with functionally viable sperm, the quality of the male gamete can influence early embryonic development, affecting processes such as embryonic gene activation, blastocyst formation, and fetal development at later stages (ZHOU W, et al., 2024). These factors are particularly relevant in post-infection contexts where sperm alterations may not prevent fertilization but subtly affect embryonic development. After fertilization, the zygote undergoes successive cleavage divisions to form the embryo, progressing through the morula, blastula, gastrula, and early fetal formation stages (RUGG-GUNN P, MORIS N, and TAM PP, 2023). Endochondral ossification begins in the seventh week of human gestation (HERRING SW, 2008) and around days 14 to 15 in mice (ORTEGA N et al., 2004), representing critical periods for the action of exogenous agents.

Fetal development assessment revealed a reduction in the number of ossification centers in the sternum compared to placebo and immunosuppressed groups, indicating that Zika virus infection, as well as other arboviruses, may alter bone development beyond the cranium, as reported in the literature (CAETANO et al., 2024). Such alterations may result from osteoblast dysfunction, as these cells are susceptible to arboviruses, demonstrated in in vitro models (MUMTAZ N, et al., 2022). Although these changes did not reflect in fetal body morphometry, impairment in ossification centers may delay or compromise skeletal development (YEKELER et al., 2003). The sternum exhibits unique features in its formation, consisting of segments called sternebrae that fuse to form a single bone, originating from the bilateral fusion of two mesenchymal cell bars (HIRASAWA T and KURATANI S, 2015). Alterations in the sternum can cause respiratory and cardiac issues due to the reduction in the thoracic cavity, which compresses vital organs such as the lungs and heart (STORONI et al., 2021).

CONCLUSION

We conclude that although Zika virus infection did not significantly impair the fertility of immunosuppressed male mice, notable alterations were observed in the skeletal development of the offspring, particularly a reduction in ossification centers of the sternum. These findings suggest that parental infection, even if it does not directly affect fertilization capacity, can hurt embryonic development. This evidence highlights the importance of considering the impact of viral infection on the paternal component of reproduction, which is frequently overlooked in studies of viral teratogenesis. Moreover, the experimental model employed proves

promising for future investigations into the molecular mechanisms underlying the interaction between the virus, spermatogenesis, and fetal development, as well as for testing therapeutic strategies aimed at preventing reproductive and embryonic damage associated with arboviral infections.

ACKNOWLEDGMENTS AND FUNDING

We thank Professor Enelise Katia Piovesan from the Institute of Petroleum and Energy Research at the Federal University of Pernambuco (LITPEG/CTG/UFPE) for providing part of the infrastructure necessary to carry out the analyses performed in this study. This study was partially funded by the Coordination for the Improvement of Higher Education Personnel (CAPES) and the Research Support Foundation of the State of Minas Gerais (FAPEMIG- BPD 00733-22).

REFERENCES

1. BROGUEIRA P, MIRANDA AC. Vírus Zika: Emergência de um Velho Conhecido Zika Virus. Revista de Sociedade Portuguesa de Medicina Interna, 2017.
2. BUSNELLI A, et al. Sperm DNA fragmentation and idiopathic recurrent pregnancy loss: results from a multicenter case–control study. Andrology, 2023; 11(8).
3. CAETANO CCS, et al. Mechanistic insights into bone remodelling dysregulation by human viral pathogens. Nature Microbiology, 2024; 9: 322–335.
4. CALVET GA, et al. Study on the persistence of Zika virus (ZIKV) in body fluids of patients with ZIKV infection in Brazil. BMC infectious diseases, 2018; 18.
5. CHAN, JFW, et al. Zika Virus Infection in Dexamethasone-immunosuppressed Mice Demonstrating Disseminated Infection with Multi-organ Involvement Including Orchitis Effectively Treated by Recombinant Type I Interferons. eBioMedicine, 2016; 14: 112 – 122.
6. DIAS FCR, et al. How bad is brazilian ginseng extract for reproductive parameters in mice? Histol Histopathol, 2020; 35(10).
7. DIAS FCR, et al. Pfaffia glomerata polyploid accession compromises male fertility and fetal development. J Ethnopharmacol, 2023; 314.
8. DIMASUAY KG, et al. Placental Responses to Changes in the Maternal Environment Determine Fetal Growth. Front Physiol, 2016; 7(12).
9. DOMINGO, E. Mechanisms of viral mutation. Cell and Molecular Life Sciences, 2016; 73(23): 4433–4448.
10. DUARTE G, et al. Zika virus infection in pregnant womanand microcephaly. Rev. Bras. Ginecol.Obst. 2017; 39(5).
11. FAISAL K, AKBARSHA MA. Control of sperm quality in the epididymis by disintegration and removal–A transmission electron microscopy study of abnormal sperm of aflatoxin-treated rat. Journal of Reproductive Healthcare and Medicine, 2024; 5(4).
12. GOVERO J, et al. Zika virus infection damages the testes in mice. Nature, 2016; 540: 438–442.
13. GUO Y, et al. Correlation between viral infections in male semen and infertility: a literature review. Virology Journal, 2024; 21(167).
14. Herring SW. Musculoskeletal system development. In: Knobil and Neill's Physiology of Reproduction. 2008
15. HEBLING MN, et al. Zika virus infection in BALB/c mice causes transient subclinical testicular damage. Animal Reproduction, 2024; 21(1): e20230124.
16. HIRASAWA T, KURATANI S. Evolution and development of the vertebrate sternum. Journal of Experimental Zoology Part B: Molecular and Developmental Evolution, 2015; 324(4): 287-297.
17. International Comitee on Taxonomy of Viruses. Disponível em: https://ictv.global/. Acesso em: 28 de maio de 2025.
18. LAPORTA GZ, et al. Global Distribution of *Aedes aegypti* and *Aedes albopictus* in a Climate Change Scenario of Regional Rivalry. Insects, 2023; 14(49).
19. LI G. et al. Characterization of cytopathic factors through genome-wide analysis of the Zika viral proteins in fission yeast. Proc Natl Acad Sci, 2017; 114.
20. MA W, et al. Zika Virus Causes Testis Damage and Leads to Male Infertility in Mice. Cell, 2017; 168: 542.

21. MCLEOD MJ. Differential staining of cartilage and bone in whole mouse fetuses by alcian blue and alizarin red S. Teratology, 1980 Dec;22(3):299-301.
22. MENDES, CF. Efeito do extrato de Mikania glomerata Sprengel (Guaco) sobre a implantação e o desenvolvimento embrionário e placentário em camundongos. Dissertação (Mestrado em Biologia Celular e Tecidual). Instituto de Ciências Biomédicas, Universidade de São Paulo, 2012.
23. MUMTAZ N. et al. Zika virus infects human osteoclasts and blocks differentiation and bone resorption. Emerging Microbes & Infections, 2022; 11(1): 1621–1634.
24. OLIVEIRA TRDP, et al. Consequences of the modulation of gestational resistance training intensity for placental cell composition and nutrient transporter expression. Placenta, 2025.
25. ORGANIZAÇÃO MUNDIAL DA SAÚDE (OMS). *Manual para análise e processamento de sêmen humano*. 6. ed. Genebra: OMS, 2021.
26. ORTEGA N, et al. Osteoblast-specific overexpression of TGF-β1 blocks bone formation and causes osteopenia by a non-cell-autonomous mechanism. Developmental Cell, 2004; 6(1): 109–120.
27. RAY P, et al. Transcriptional signatures throughout development: the effects of mouse embryo manipulation in vitro. Reproduction, 2017; 153(1): 107–118.
28. RUGG-GUNN PJ, et al. Early human development and stem cell-based human embryo models. Development, Cambridge, 2023; (150): 201797.
29. SANTOS J, MENESES BM. An integrated approach for the assessment of the Aedes aegypti and Aedes albopictus global spatial distribution, and determination of the zones susceptible to the development of Zika virus. Acta Trop, 2017; 168.
30. SILVA AA. A infecção pelo vírus Zika causa alterações morfológicas testiculares e espermáticas em camundongos balb/c adultos. Dissertação (Mestrado em Biologia Aplicada à Saúde) - Instituto Keizo Asami. Universidade Federal de Pernambuco, Recife, 2020.
31. SHENG ZY, et al. Sertoli cells are susceptible to ZIKV infection in mouse testis. Frontiers in Cellular and Infection Microbiology, 2017; 7.
32. STORONI S, et al. Pathophysiology of respiratory failure in patients with osteogenesis imperfecta: a systematic review. Annals of Medicine, 2021; 53(1): 1676–1687.
33. URAKI R, et al. Zika virus causes testicular atrophy. Sci. Adv, 2017; (3).
34. VERNET P, et al. Antioxidant strategies in the epididymis. Mol Cell Endocrinology, 2004; 216.
35. WAI-SUN O, et al. Male genital tract antioxidant enzymes-Their ability to preserve sperm DNA integrity. Molecular and Cellular Endocrinology, 2006; 250(2).
36. WATANABE S, VASUDEVAN SG. Clinical and experimental evidence for transplacental vertical transmission of flaviviruses. Antiviral research, 2023; 210.
37. Wu KY, et al. Vertical transmission of Zika virus targeting the radial glial cells affects cortex development of offspring mice. Cell research, 2016; 26(6): 645-654.
38. YEKELER E, et al. Pseudomass of the sternal manubrium in osteogenesis imperfecta. Skeletal Radiology, 2003; 32(6): 371–373.
39. ZHANG Y, et al. Zika Virus Infection in the Ovary Induces a Continuously Elevated Progesterone Level and Compromises Conception in Interferon Alpha/Beta Receptor-Deficient Mice. J Virol., 2022; 96: e01189-21.
40. ZHOU W, et al. Mean number of DNA breakpoints: Illuminating sperm DNA integrity and in vitro fertilization outcomes. Fertility and Sterility, 2024; 121(2): 264-270.